Clays and Clay Minerals, Vol. 53, No. 3, 268–277, 2005.

CASTOR TOXIN ADSORPTION TO CLAY MINERALS

WILLIAM F. JAYNES[1,*], RICHARD E. ZARTMAN[1], CARY J. GREEN[1], MICHAEL J. SAN FRANCISCO[2] AND JOHN C. ZAK[2]

[1] Plant and Soil Science Department and [2]Biological Sciences Department, Texas Tech University, Lubbock, Texas 79409, USA

Abstract—The extremely toxic protein, ricin, is derived from castor beans and is a potential terrorist weapon. Adsorption to clays might minimize the environmental persistence and toxic effects of this toxin. Ricin adsorption to clay minerals was measured using batch adsorption isotherms. Enzyme-linked immunoassay methods were used to quantify aqueous ricin concentrations. Montmorillonite, sepiolite and palygorskite effectively adsorbed ricin from aqueous solutions and yielded mostly Langmuir-type isotherms. The monolayer adsorption capacity from a Langmuir equation fit at pH 7 was 444 g ricin/kg for montmorillonite (SWy-2), but was only 5.6 g ricin/kg for kaolinite (KGa-1b). Monolayer capacities for sepiolite (SepSp-1) and palygorskite (PFl-1) at pH 7 were 59.2 and 58.1 g ricin/kg. The high-charge montmorillonite (SAz-1) effectively adsorbed ricin at pH 7, but yielded a linear isotherm with K = 5530 L/kg. At pH 5, both montmorillonites (SWy-2 and SAz-1) yielded Langmuir-type isotherms with monolayer capacities of 694 and 641 g ricin/kg. Clay samples with higher cation exchange capacities generally adsorbed more ricin, but adsorption also followed specific surface area. X-ray diffraction of <2 μm SWy-2 treated with 470 g ricin/kg indicated expansion up to 34.6 Å at buffered pHs of 4 and 7, but not at pH 10. Furthermore, ricin adsorption was greatest at pH 4 and 7, but minimal at pH 10. Treatment with 1.41 kg of purified ricin/kg clay at pH 5 yielded a 35.3 Å peak and adsorption of ~1.2 kg ricin/kg. Similar treatment with lower-purity ricin yielded less expansion and lower adsorption. The 35.3 Å peak interpreted either as a d_{002} or d_{001} reflection indicates a 70.6 Å or a 35.3 Å ricin/SWy-2 complex. This implies that adsorption and air drying have compressed interlayer ricin molecules by 18 to 65%. Effective ricin adsorption by montmorillonite suggests that it could be used to minimize the toxic effects of dispersed ricin.

Key Words—Adsorption, Cation Exchange Capacity, Kaolinite, Lectin, Montmorillonite, Palygorskite, pH, Protein, Ricin, Sepiolite, Specific Surface Area.

INTRODUCTION

The ricin toxin is found in the seeds of the castor plant (*Ricinus communis*) that is extensively cultivated to produce castor oil. Castor beans contain 1–5% ricin by weight (Franz and Jaax, 1997). Ricin is one of the most toxic compounds known and ingestion of castor beans can produce serious poisoning and death (Merck, 2001). It has recently gained notoriety due to its use in political assassinations and as a terrorist weapon (Owens, 2000). There is, however, great interest in ricin as a potential antitumor agent in cancer research (Nicolson and Blaustein, 1972; Montfort *et al*., 1987). Ricin's potential both as a weapon and an antitumor agent is due to its toxicity to cells by inhibiting protein synthesis in the ribosomes (Olsnes and Pihl, 1973). Ricin is a globular protein and a lectin. A lectin is a protein of non-immune origin that agglutinates cells and/or precipitates complex carbohydrates (Sigma, 2000).

Lectins are widely distributed in nature and even occur in edible legumes such as kidney beans, lima beans, soybeans, peanuts, lentils, peas and many other plants (*e.g.* avocado, potato, tomato, wheat) that are commonly consumed in human diets (Liener, 1997). The physiological role of lectins in plants is unknown but these proteins might act as a defense mechanism against predators and plant viruses or as mediators in symbiotic relationships with nitrogen-fixing bacteria (Liener, 1997; Hartley and Lord, 1993). Liener (1997) noted that lectins interfere with the adsorption of nutrients by binding to glycoproteins on the microvilli lining of the small intestine and that other toxic effects result from lectin entry into the circulatory system. Experiments demonstrating that the nutritive value of soybeans was increased by heat treatment were the first sign that lectins can act as anti-nutrients (Liener, 1997). Several incidents of severe gastroenteritis caused by the lectins in uncooked kidney beans have been reported (Liener, 1997). Heat treatment denatures proteins and effectively removes the toxic and anti-nutrient properties of lectins.

Ricin is a protein which is a polymer formed by peptide bonds between amino acids. Twenty different amino acids are commonly found in proteins and these amino acids differ in the composition of the side chains (Stryer, 1975). The amino acid residues in proteins, such as ricin, have amine, carboxylic acid, alkyl, aromatic and other functional-group side chains that affect the properties. In particular, the amino and carboxylic acid side chains cause the net charge and solubility to vary with

* E-mail address of corresponding author:
william.jaynes@ttu.edu
DOI: 10.1346/CCMN.2005.0530306

pH. The A and B chains of ricin overall contain 529 amino acid residues (Katzin *et al*., 1991; Rutenber and Robertus, 1991) of which 42 contain acidic side chains (aspartate and glutamate) and 43 contain basic side chains (histidine, lysine and arginine). The isoelectric point of a protein (ricin = 7.1) is the pH where the molecule has a net charge of zero (Merck, 2001). Solution pHs that maximize cationic groups should maximize adsorption to high cation exchange capacity (CEC) materials and conversely, pHs that maximize anionic groups should minimize adsorption. Clay mineral surface acidity could protonate side-chain amine groups and might also affect adsorption (Mortland and Raman, 1968; Rausell-Colom and Serratosa, 1987).

The ricin molecule has a complex structure consisting of a ~32 kDa A chain linked by a disulfide bond to a ~32 kDa B chain (Figure 1). The A chain contains 267 amino acid residues and the B chain contains 262 (Rutenber *et al*., 1991). The A chain is ~55 Å long, 45 Å wide and 35 Å thick. The A chain folds into three substructures that contain a five-stranded β-sheet, five α-helices and a disc-like domain, respectively. The B chain is ~70 Å long and 30 Å wide and consists of two separate, almost-spherical folding domains which are ~30 Å thick. The two domains of the B chain each contain two disulfide loops that can each bind to one lactose molecule (Montfort *et al*., 1987). Hence, the B chain confers the sugar-residue binding properties to ricin.

Olsnes and Pihl (1973) showed that the A chain in ricin is toxic because it prevents protein synthesis, whereas the B chain is essentially non-toxic and acts to bind the molecule to a cell surface. In this respect, Olsnes and Pihl (1973) reported similarities between ricin, abrin and diphtheria toxins in that each toxin molecule has a toxic part and a part that binds the molecule to a cell surface. They also showed that the separate A chain prevents protein synthesis in ribosomes isolated from cells, but not in ribosomes inside cells. To inactivate ribosomes inside cells, the ricin A chain requires the B chain to bind to the cell surface and facilitate entry into the cell.

Several research articles have reported that clays effectively adsorb amino acids and proteins. Goh (1972) reported that amino acids adsorbed to New Zealand soil profiles were persistent and could be used in paleosol identification (*i.e.* buried former surface horizons). Rausell-Colom and Fornes (1974) and Fu *et al*. (1996) used cation exchange to prepare vermiculite and saponite/amino acid complexes. Garwood *et al*. (1983) found that Na-montmorillonite effectively adsorbed the

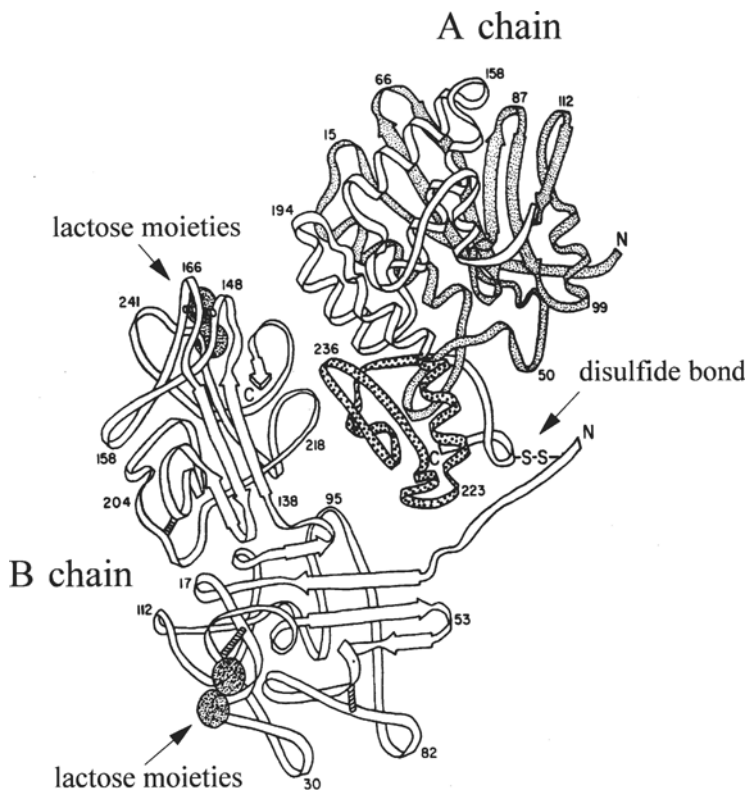

Figure 1. Ribbon depiction of ricin structure. Disulfide bond linking A and B chains shown at center right. Numbers identify positions of amino acids. A-chain sequential parts are shaded and B-chain lactose moieties denoted by the discs. After Montford *et al*. (1987).

https://doi.org/10.1346/CCMN.2005.0530306 Published online by Cambridge University Press

enzyme, glucose oxidase, at pH values below the isoelectric point. Perez-Castells *et al.* (1985) examined adsorption of collagen (a fibrous protein) by sepiolite. They reported that sepiolite adsorbed 0.4 mg of collagen/mg of clay at pH 4 and concluded that even higher loadings of collagen could be achieved. Perez-Castells *et al.* (1985) concluded that the bonding between clay and protein must be electrostatic because pH and ionic strength affected adsorption. Ding and Henrichs (2002) examined the adsorption and desorption of proteins and polyamino acids by montmorillonite, illite, goethite and marine sediments. They concluded that montmorillonite, illite, goethite and marine sediments strongly and rapidly adsorbed proteins and that much of the adsorbed protein was not readily desorbed. In adsorption experiments, much greater adsorption of basic rather than acidic polyamino acids was observed. This led Ding and Henrichs (2002) to conclude that electrostatic (*i.e.* coulombic) interactions were dominant in protein adsorption.

The CEC and large surface area of clay minerals could make them effective sorbents for toxic proteins. Adsorption of ricin and other toxic proteins by clay minerals might effectively immobilize these toxins and reduce or eliminate the toxicity. This could be important in a terrorist incident after intentional dispersal of a toxin. Useful applications for clays might be found in minimizing the toxic effects of ricin and other poisonous lectins. Hence, the objectives of this study were to measure ricin adsorption by a variety of clay minerals, determine whether adsorption causes interlayer expansion, and examine pH, CEC and specific surface-area effects on adsorption. From these data, likely mechanisms involved in ricin adsorption and factors that enhance or reduce adsorption might be learned. Such data would be a useful guide in contaminated-site cleanup and in understanding the environmental fate of ricin.

MATERIALS AND METHODS

Reference clay mineral samples were obtained from the Source Clays Repository of The Clay Minerals Society, currently housed at Purdue University, West Lafayette, Indiana. The clay samples used in this study were SWy-2, SAz-1, SepSp-1, PFl-1 and KGa-1b. Clays were selected based on ubiquity in soils/sediments, availability and potential effectiveness as sorbents. Montmorillonite and palygorskite effectively sorb a variety of substances and are readily available in pet litter, oil sorbents and other commercial products. Sepiolite and kaolinite are used as carriers in pharmaceuticals. The <2 μm fraction of SWy-2 was separated using gravity sedimentation for use in the X-ray diffraction (XRD) studies. The clay samples were mostly used as received for the adsorption isotherms. However, samples of SWy-2 and SAz-1 were Na^+ saturated and dispersed in water to deliver more accurately the small amounts (3–10 mg) used in the adsorption isotherms. Properties of the clay minerals are listed in Table 1. The CEC values, obtained from Jaynes and Bigham (1986), are comparable to those reported by van Olphen and Fripiat (1978). Clay contents were measured using the hydrometer method (Bouyoucos, 1962).

Surface-area measurements

Nitrogen surface areas were measured by the single-point method using a Micromeritics Flowsorb II model 2300 surface area meter with a carrier gas containing 30% N_2 and 70% He. These external surface areas are comparable to those reported by van Olphen and Fripiat (1979) for the reference clays. The ethylene glycol monoethyl ether (EGME) method of specific surface-area measurement was also used (Carter *et al.*, 1986, method 16-3). The EGME method is a measure of total specific surface area because EGME can penetrate into the interlayers of expandable clays and the channels of fibrous clays. Because the N_2 cannot penetrate into collapsed interlayers, gas adsorption methods only measure the external surface area of expandable clays.

Preparation of ricin stock solution

Castor beans were obtained from a local seed company. Nicolson and Blaustein (1972) discussed a method to extract ricin from castor beans. Using a similar procedure, castor oil was extracted with acetone from castor beans minced to <2 mm using a nut chopper. The castor oil/acetone supernatant liquid was decanted and discarded. The residual acetone in the castor bean residue was evaporated under a hood. An aqueous ricin stock solution was prepared by extracting the castor bean residue with phosphate-buffered saline solution, pH 7.4

Table 1. Properties of silicate clay minerals.

Sample/ mineralogy	Source clay name from The Clay Minerals Society	% Clay	N_2 external surface area (m^2/g)	EGME total surface area (m^2/g)	CEC (cmol/kg)
Montmorillonite	SWy-2	90	27	630	80
Montmorillonite	SAz-1	85	76	761	125
Sepiolite	SepSp-1	90	317	452	17
Palygorskite	PFl-1	85	178	334	20
Kaolinite	KGa-1b	75	11	12	2

https://doi.org/10.1346/CCMN.2005.0530306 Published online by Cambridge University Press

containing 0.1% sodium azide added to inhibit microbial activity (PBSZ). Phosphate-buffered saline (PBS) contains 0.01 M KH_2PO_4, 0.138 M NaCl and 0.0027 M KCl. Castor beans contain two lectins, designated RCA_{60} and RCA_{120} by their approximate molecular weights of 60 kDa and 120 kDa; RCA_{60} is the ricin toxin and RCA_{120} is an agglutinin (Sigma, 2000). Hence, the ricin stock solution contains both lectins and other soluble components of the bean. A centrifuge and 0.45 μm filters were used to remove suspended matter. A small quantity of purified ricin solution was obtained from Southwestern Medical Center (SWMC) in Dallas, Texas and was used in the XRD studies of oriented samples of <2 μm SWy-2.

Total protein (TP) by the Bradford (1976) method and ELISA measurement of RCA_{60} content were made to compare the purity of the different ricin samples. The Sigma RCA_{60} standard contained 3.9 mg/mL TP and 3.9 mg/mL RCA_{60}. The SWMC sample contained 4.0 mg/mL TP and 2.8 mg/mL RCA_{60}. The ricin stock solution contained 51.5 mg/mL TP and 5.1 mg/mL RCA_{60}. Hence, the SWMC purified ricin sample was almost as pure as the Sigma standard, but only 10% of the total protein in the ricin stock solution was ricin.

ELISA measurement of ricin

Ricin concentrations were measured using an enzyme-linked immunosorbent assay (ELISA) method. A modification of a generic indirect ELISA method in the Sigma 2000/2001 catalog was used to measure ricin concentrations (Boroda *et al.*, 2004). Purified ricin (RCA_{60}) was obtained from Sigma and used as the standard. Rabbit anti-ricin antibody and goat anti-rabbit antibody with attached horseradish peroxidase enzyme were also obtained from Sigma. Ricin standards were prepared by dilution into PBSZ to yield concentrations from 1 to 50 ng/mL (ppb). The typical detection limit was ~2 ng/mL with ±10% precision. The method is specific for $RCA_{60;}$ RCA_{120} and other proteins are not detected. Standard ricin and sample solutions were diluted with PBSZ and pipetted into wells of the microplates. The microplates with diluted ricin standards and samples were incubated at 37ºC for 2 h to attach ricin to the walls of the microplate wells. Between treatments, the microplates were washed three times with phosphate-buffered saline solution, pH 7.4, containing 0.05% Tween 20 (PBST). The microplates were treated with bovine serum albumin (BSA), 2.5% in PBST to prevent non-specific adsorption to the microplate. The plates were then treated with a solution containing an antibody for ricin (RCA_{60}) developed in rabbits. Next, the plates were treated with a solution containing an antibody to rabbit proteins developed in goats with an attached horseradish peroxidase enzyme molecule. In the final step, a substrate solution for the enzyme was added to the microplates. The enzyme in the goat anti-rabbit/rabbit anti-ricin/ricin 'sandwich' catalyzes color development in the substrate solution. Color development is proportional to the enzyme concentration that in turn is proportional to the ricin concentration. Absorbance of the colored solutions in the microplates was used to calculate ricin concentrations based on the absorbance of the ricin standard samples.

Ricin adsorption isotherms

Batch adsorption isotherms were prepared by adding aliquots of the ricin stock solution to weighed samples of the reference clays in centrifuge tubes. To deliver the small weights more accurately, 0.40 g samples of SWy-2 and SAz-1 were Na^+ saturated, ultrasonically dispersed in 20 mL of deionized water and 0.50 mL (10 mg) or 0.15 mL aliquots (3 mg) were pipetted into the tubes. The samples of SepSp-1, PFl-1 and KGa-1b were directly weighed into centrifuge tubes. Six point isotherms were prepared in duplicate for SWy-2 (10 mg), SAz-1 (10 mg), SepSp-1 (50 mg), PFl-1 (50 mg) and KGa-1b (500 mg) by pipetting 0.1, 0.2, 0.4, 0.6, 0.8 and 1.0 mL aliquots of the ricin stock solution (~5.1 mg ricin/mL), 0–0.9 mL PBSZ and 19 mL of deionized water for a total volume of 20 mL. The 0–0.9 mL of PBSZ were added to make the volume of PBSZ equal to 1.0 mL for all samples and to buffer the pH to ~7. The other clay mineral samples were ultrasonically dispersed in water before addition of PBSZ or ricin stock solution. Blanks were prepared similarly except without a clay mineral sample. Adsorption isotherms were prepared at pH 5 for SWy-2 (3 mg) and SAz-1 (3 mg) using 19 mL of a pH 5 buffer instead of the deionized water. Adsorption isotherm plots were constructed by graphing the amounts of ricin adsorbed per unit sample weight *vs.* the ricin concentrations in the equilibrium solutions. Adsorbed ricin was calculated from the difference between the ricin concentrations in the sample and the blanks. Ricin adsorption per unit weight of clay was calculated by dividing the amount adsorbed by the sample weight. The isotherms (except SAz-1, pH 7) were fitted to the Langmuir equation (r^2 values >0.97) and estimated monolayer adsorption capacities (*Xm*) were calculated (Hiemenz, 1986). Because the SAz-1 isotherm at pH 7 was linear (r^2 = 0.97) and did not fit Langmuir (r^2 <0.45), the *K* value or slope of the line was calculated instead of *Xm*.

Preparation of oriented ricin/clay complexes

Six dispersed samples of <2 μm SWy-2 that contained 36.4 mg of clay were pipetted onto each of six 47 mm diameter 0.45 μm cellulose nitrate membrane filters. Vacuum was used to attach and orient the clay particles to the membrane filters. Buffer solution concentrates were obtained from Fisher Scientific. Solutions (10 mL) containing the buffer (pH 4, pH 7, pH 10) and ricin (~17.1 mg) were added to three of the oriented clay samples. Controls containing only the buffer (pH 4, pH 7,

pH 10) were prepared using the other three oriented clay samples. Vacuum was used to pass the ricin/buffer solutions through the oriented clay samples. After the buffer solutions were passed through the clays, three deionized-water washes (~3 mL each) were used to remove excess salts and non-adsorbed ricin from the clays. The membrane filters with attached oriented clay samples were removed from the filter holders and attached to glass slides using double-sticky tape. The filtrates (ricin/buffer plus water washes) collected from the clay samples were transferred to plastic vials and the volumes adjusted to the same volume.

Similarly, two ricin-treated <2 μm SWy-2 samples were prepared at pH 5, one using purified ricin and the other using ricin stock solution. For the purified ricin-treated sample (36.4 mg), three times as much ricin (~51.2 mg) was used to achieve a greater ricin loading on the clay. The clay sample (36.4 mg SWy-2) oriented on a 47 mm membrane filter was leached with purified ricin solution and washed with deionized water. After leaching with the purified ricin/buffer solution, the membrane filter was mounted on a glass slide and saved for later XRD analysis. The filtrate was saved for later ricin analysis. The other SWy-2 sample (42 mg) was treated with 12 mL of ricin stock solution (~61 mg of ricin) in 228 mL of pH 5 buffer along with a blank containing only ricin stock solution and buffer. After shaking for 2 h, the SWy-2 sample and blank were centrifuged and the supernatant liquids saved for later ricin analysis. The sedimented material from the SWy-2 sample and blank were dispersed in water and collected on 47 mm membrane filters, air dried overnight and weighed. After drying and weighing, ~30 mg of the SWy-2 sample treated with ricin stock solution were dispersed in water and dried on a glass slide. Ricin concentrations and pH were later measured on the filtrates. The oriented clay samples were left overnight or longer to air dry under a hood. X-ray diffraction patterns were collected for the oriented clays by scanning from 2 to 30°2θ using CuKα radiation and a Philips diffractometer interfaced to a computer.

RESULTS AND DISCUSSION

The low-charge montmorillonite, SWy-2, effectively adsorbed ricin with a calculated monolayer capacity of 444 g ricin/kg (Figure 2). Most of the isotherms were of the Langmuir type. Fusi *et al.* (1989) similarly found that adsorption of the proteins, catalase and β-lactoglobulin, to clays generally produced isotherms of the Langmuir type. The higher-CEC montmorillonite (SAz-1) did not adsorb as much ricin at pH 7 as the other montmorillonite (SWy-2) and was not as effective a ricin sorbent (Figure 2). Because the SAz-1 isotherm did not fit the Langmuir equation, a comparison of monolayer capacities cannot be made. The SAz-1 isotherm data were instead fitted to a line (r^2 = 0.97) and a K value of 5530 L/kg was calculated.

Another set of isotherms for SWy-2 and SAz-1 were prepared using pH 5 buffer with only 3 mg samples in order to permit greater ricin loading (Figure 3). Both clay mineral samples yielded Langmuir-type plots with similar calculated monolayer capacities of 694 and 641 g ricin/kg. It is not clear why the SAz-1 sample yielded a linear plot at pH 7 (Figure 2) and a Langmuir-type plot at pH 5 (Figure 3). However, limited aqueous expansion of the high-charge clay and uncharged or weakly-charged ricin molecules near the isoelectric point might have limited adsorption.

The large internal surface areas of montmorillonites are not included in the N_2 'external' surface area values in Table 1. The dry conditions required for N_2 surface-area measurements collapse the interlayers in expandable clays. The larger EGME 'total' surface area values include interlayer surfaces and are a better indication of montmorillonite surfaces available to aqueous sorbates.

Both of the fibrous clay mineral samples (SepSp-1 and PFl-1) effectively adsorbed ricin with monolayer

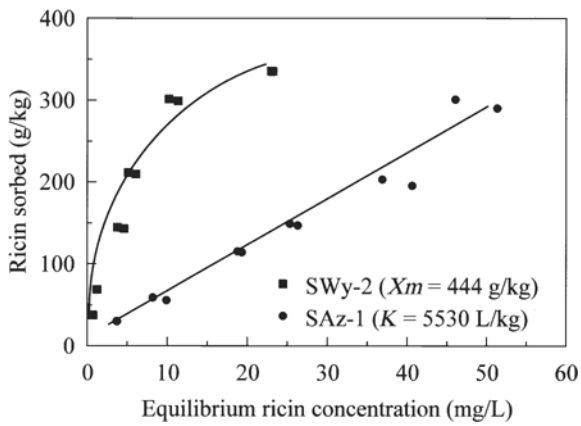

Figure 2. Ricin adsorption to montmorillonites at pH 7; monolayer adsorption capacity based on Langmuir fit and K-value based on linear fit.

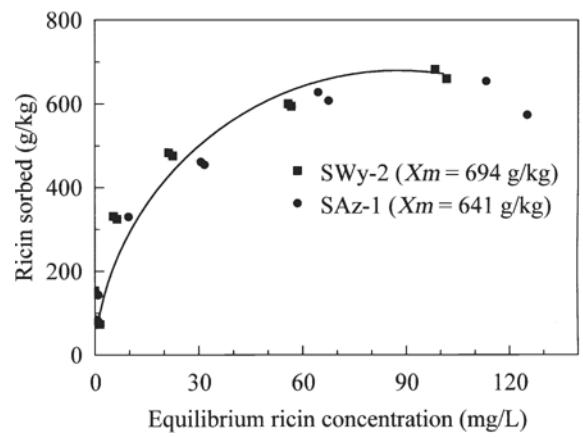

Figure 3. Ricin adsorption to montmorillonites at pH 5; monolayer adsorption capacities based on Langmuir fit.

https://doi.org/10.1346/CCMN.2005.0530306 Published online by Cambridge University Press

capacities of ~59 g/kg for sepiolite and palygorskite (Figure 4). Much of the surface areas of sepiolites and palygorskites, however, are from micropores inside the channels that might be accessible to N_2 and EGME, but are much too small for ricin. Singer (2002) reported that 60–70% of the surface area in sepiolites and palygorskites was due to micropores. Hence, the potential surface area accessible to ricin in the palygorskite and sepiolite samples was probably only ~130–180 m^2/g.

Ricin adsorption to the KGa-1b kaolinite (Figure 5) at pH 7 was much less than for the other clay minerals (Figures 2 and 4) with a monolayer capacity of only 5.6 g ricin/kg. The kaolinite surface area was also very small (~12 m^2/g) with comparable N_2 and EGME values. This mineral would be a much less effective ricin sorbent.

Ricin was adsorbed effectively by montmorillonite, sepiolite and palygorskite with high to moderate CECs, but much less effectively by the low-CEC mineral, kaolinite. The mineral sample CEC values parallel monolayer ricin adsorption capacities and suggest that CEC affects adsorption. However, EGME surface areas also correlate with ricin adsorption capacities, especially if the sepiolite and palygorskite surface areas are corrected for inaccessible micropores.

The monolayer ricin adsorption capacities for clay minerals, even for kaolinite (~6 g/kg), were high relative to many sorbents and indicate strong adsorption. Fusi *et al*. (1989) also concluded that clays strongly adsorb proteins. The *K* value of 5530 for ricin adsorption to SAz-1 at pH 7 is comparable to the 4818 *K* value for naphthalene sorption to the organoclay, SAz-HDTMA (Jaynes and Boyd, 1991).

Ding and Henrichs (2002) corrected the Rubisco protein adsorption *K* values because protein was adsorbed by the glass containers used in the study. Similar problems with ricin adsorption to sample containers were observed in this study and were corrected in the isotherms using blanks. Norde (2003) noted that polymer adsorption occurs ubiquitously and that among biopolymers, proteins are the most surface-active. New polypropylene centrifuge tubes and silanized-glass containers were used when possible to minimize adsorption to containers.

XRD of ricin/SWy-2 complexes

X-ray diffraction patterns of the pH 10 buffer-treated SWy-2 samples in Figure 6a are very similar. No expansion of SWy-2 with ricin at pH 10 is evident. In contrast, diffraction patterns of the pH 4 and pH 7 buffer-treated samples expanded after ricin treatment (Figure 6b,c). The buffer solutions all contained K and/or Na salts: pH 4, $KHC_8H_4O_4$; pH 7, KH_2PO_4 and NaOH; and pH 10, H_3BO_3, KCl and NaOH. The SWy-2 samples treated only with the pH 4, 7 and 10 buffer solutions yielded basal spacings of 11.8–12.2 Å consistent with K^+- and Na^+-saturated montmorillonites (MacEwan and Wilson, 1980). The SWy-2 sample treated with pH 7 buffer and ricin yielded a broad peak at 21.2 Å. The SWy-2 sample treated with pH 4 buffer and ricin yielded a sharp peak at 34.6 Å, a broad peak near 23.1 Å and a sharp peak at 12.2 Å. The broadness of the peak at 21.2 Å suggests that it represents an interstratification between SWy-2 interlayers containing different amounts of ricin. In contrast, the sharp peak at 34.6 Å suggests that it might represent a single phase. Interpreting the 34.6 Å peak as a d_{002} value (*i.e.* d_{001} = 69.2 Å) and using 9.6 Å as the thickness of a collapsed montmorillonite layer suggests an interlayer expansion of 59.6 Å. Unfortunately, our X-ray diffractometer cannot operate at the low 2θ angles (<2°2θ) needed to resolve directly such large spacings.

Villafranca and Robertus (1977) determined the crystal structure of ricin to be orthorhombic space group $P2_12_12_1$ with unit-cell dimensions a = 72.9 Å, b = 79.1 Å and c = 114.7 Å. The ricin crystals used by Villafranca and Robertus (1977) were grown from an aqueous solution containing 6% polyethylene glycol, 0.002 M lactose and 0.05 M acetate buffer at pH 4.75. The unit-cell contains four asymmetric ricin molecules and 52% solvent

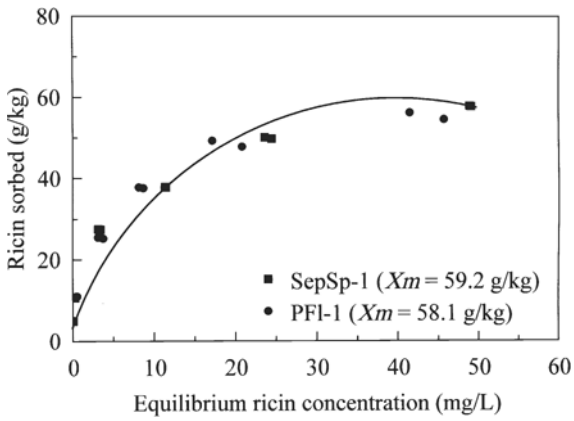

Figure 4. Ricin adsorption to sepiolite and palygorskite at pH 7: monolayer adsorption capacities based on Langmuir fit.

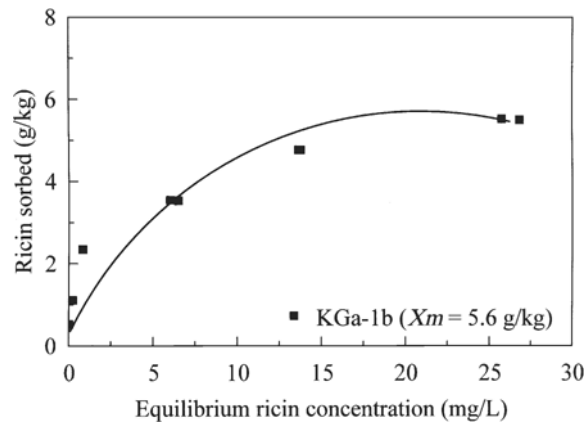

Figure 5. Ricin adsorption to kaolinite at pH 7; monolayer adsorption capacity based on Langmuir fit.

https://doi.org/10.1346/CCMN.2005.0530306 Published online by Cambridge University Press

molecules (*i.e.* water). The expected basal spacing for interlayer ricin adsorbed with the *a* axis perpendicular to the montmorillonite interlayer would be 72.9 + 9.6 = 82.5 Å. An interlayer expansion of only 59.6 Å implies an 18% decrease in the ricin *a* dimension. Conversely, interpretation of the 34.6 Å spacing as a d_{001} reflection would suggest a 66% decrease in the ricin *a* dimension. An 18% decrease in the ricin *a* dimension after adsorption and air drying seems reasonable due to the 52% water content in the ricin unit-cell. Likewise, Montfort *et al.* (1987) noted that changes in ricin unit-cell parameters caused by variations in humidity had frustrated their efforts to derive a three-dimensional structure. Similarly, based on molecular dynamics simulations, Yu *et al.* (2000) concluded that adsorption to clay mineral surfaces might denature globular proteins and warp clay interlayers due to perturbation of the surrounding water structure and much greater expansion at protein adsorption sites.

Effect of pH on ricin adsorption by oriented <2 μm SWy-2

Ricin adsorption for the oriented clay samples (Figure 6) was calculated from the difference between the amount of ricin added and ricin recovered in the extracts. No correction was made for any ricin that might have adsorbed to the containers. The pHs of the extracts with and without added ricin were close to the buffer values of 4, 7 and 10. Most ricin added to the pH 10 sample was recovered in the filtrate and only ~75 g of ricin/kg of clay were adsorbed (Figure 6a). Far less of the added ricin was recovered in the pH 7 and pH 4 sample filtrates. The pH 7 sample adsorbed ~370 g of ricin/kg of SWy-2 (Figure 5b) and the pH 4 sample retained ~470 g of ricin/kg of SWy-2 (Figure 6c). At pH 4, the ricin molecule should mostly have positively charged sites due to protonated side-chain amine groups (*e.g.* arginine) and undissociated carboxyl groups (*e.g.* aspartic acid). At pH 7 near the isoelectric point (7.1), the ricin molecule should have about an equal number of negatively and positively charged sites (*i.e.* zwitterion). At pH 10, ricin molecules should mostly be negatively charged due to ionized carboxyl groups and neutral amine groups on the side chains. The lack of expansion and minor ricin adsorption at pH 10 suggests that the negatively charged clay surface effectively repelled ricin molecules.

Another set of buffer/ricin-treated SWy-2 <2 μm samples were prepared to attain greater ricin loading and interlayer expansion (Figure 7). For these samples, the pH was buffered at pH 5 and three times as much ricin (~1400 g/kg clay) as in Figure 6 was used to achieve a greater loading on the clay. In the upper XRD trace (Figure 7a), purified ricin was used, whereas ricin stock solution was used for the lower one (Figure 7b). The 34.6 Å peak identified in Figure 6c has shifted to 35.3 Å in Figure 7a suggesting a 70.6 Å (d_{001}) basal spacing. In this sample, a much greater ricin loading of 1200 g/kg clay was achieved. Garwood *et al.* (1983) similarly reported the adsorption of ~970 g/kg of the globular

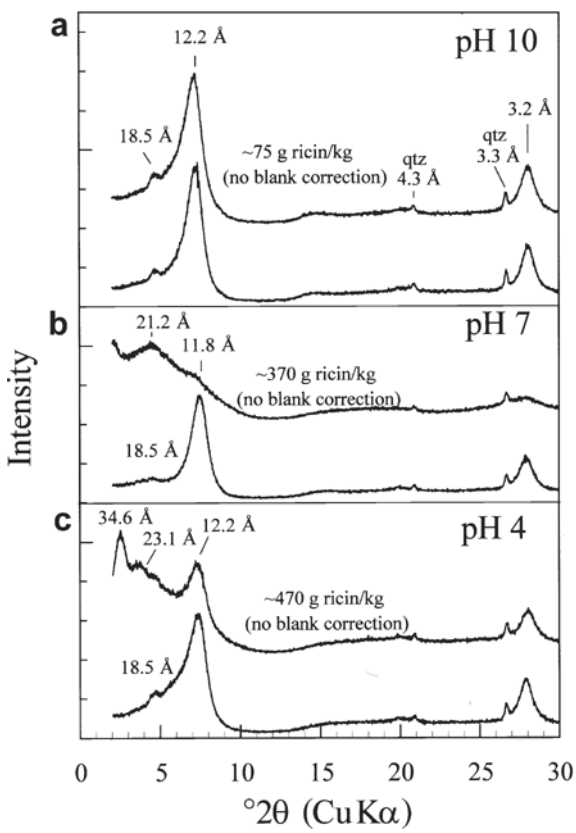

Figure 6. Purified ricin (~470 g/kg) and pH buffer effects on <2 μm SWy-2 expansion: upper traces in parts a, b, c: ricin treated; lower traces: controls; ricin adsorption estimated from filtrate recovery, no blank correction; (a) pH 10; (b) pH 7; and (c) pH 4.

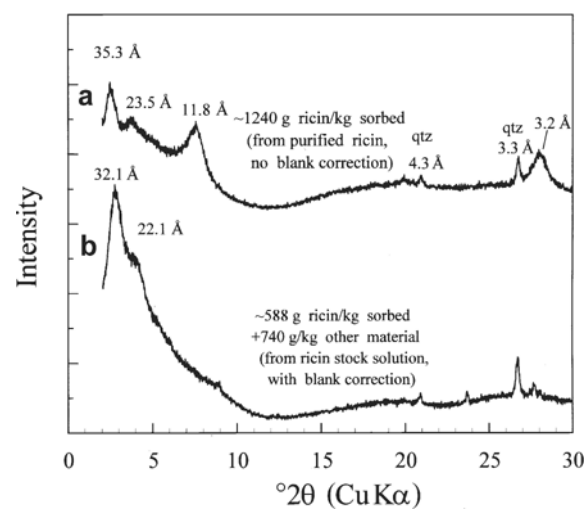

Figure 7. Greater added ricin (~1400 g ricin/kg), purity and pH 5 buffer effects on <2 μm SWy-2 expansion: (a) purified ricin, no blank correction; (b) ricin stock solution, blank correction and measured weight gain.

https://doi.org/10.1346/CCMN.2005.0530306 Published online by Cambridge University Press

protein, glucose oxidase, to Na-montmorillonite. The somewhat greater interlayer expansion in Figure 7a implies a 16% decrease in the ricin *a* dimension or a 65% decrease if the 35.3 Å peak is interpreted as a 001 reflection. In Figure 7b, there was less interlayer expansion and less ricin adsorption when the less pure ricin stock solution was used instead of the purified ricin solution.

The SWy-2 monolayer capacity of 694 g of ricin/kg (Figure 3) is only about one half of the estimated adsorption in Figure 7a, but comparable to that in Figure 7b. Two causes might account for this discrepancy. First, ricin adsorption in Figures 6 and 7a was calculated from the difference between ricin added and ricin recovered in the filtrates without any correction for ricin adsorption to the filtration containers. Blanks were used in the isotherms (Figures 2, 3, 4, 5) and in Figure 7b to correct for ricin adsorption to the containers. Secondly, the ricin used (SWMC) for Figures 6 and 7a was much purer than the ricin stock solution that was used for the isotherms. Impurities in the ricin stock solution might have limited adsorption in the isotherms (Figure 2, 3, 4, 5) and in Figure 7b. In Figure 7b, ~590 g/kg of ricin were adsorbed by SWy-2 at pH 5, but weight measurements indicate that ~1330 g/kg of material were adsorbed. Hence, ~740 g/kg of non-ricin material were also adsorbed.

A calculation can be made to determine whether montmorillonite interlayers have enough surface area to accommodate 470 mg ricin/g. Each adsorbed ricin molecule would have a siloxane surface on both sides of it in the interlayer. The four ricin molecules in a unit-cell require (*bc* plane adsorption) $79.1 \times 114.7 = 9073$ Å^2 of siloxane surface for each side of the unit-cell or $2268 \times 2 = 4536$ Å^2 for both sides of one ricin molecule. Hence, the surface area required for adsorption of 470 mg of ricin (molecular weight = 65,000 Da) would be $(4536*0.47*N_A*10^{-20}$ m^2/Å$^2)/65{,}000 = 198$ m^2, where N_A is Avogadro's number. Hence, montmorillonite interlayers might have enough room to retain three times as many ricin molecules (*i.e.* $630 \times 0.47/198 = 1.5$ g ricin/g clay). However, due to inefficient packing and other factors, adsorbed compounds often require somewhat more surface area than the dimensions of the compound would indicate.

A calculation can also be made to determine the number of charge sites in montmorillonite available to adsorbed ricin molecules. Each of the two siloxane surfaces in a unit-cell ($\sim Si_8Al_{4-x}Mg_xO_{20}(OH)_4$) of montmorillonite has a surface area of ~46.99 Å^2 based on Brindley's (1980) unit-cell values of $a = 5.21$ Å and $b = 9.02$ Å. The SWy-2 montmorillonite contains ~0.68 negative charge sites/unit-cell (Jaynes and Bigham, 1987; data on SWy-1) or 0.34 for each of the two 46.99 Å^2 siloxane surfaces. This is equivalent to a negative charge on the siloxane surfaces of 0.34/46.99 Å^2 or one negative charge site per 138 Å^2. An undistorted ricin molecule would cover 2268 Å^2 of siloxane surface on each side of a montmorillonite interlayer. Each ricin molecule would have 2268/138 = 16.4 charge sites available on each side. Due to the complex and voluminous structure of ricin (Figure 1), it is unlikely that more than a fraction of the charged sites on a ricin molecule could be in physical contact with the clay surface.

Francis (1973) noted that Wyoming bentonite retained 60% of its initial CEC after adsorption (28 g PVP/100 g clay) of the linear, nonionic, 40 kDa polymer, polyvinylpyrrolidone (PVP). Ricin adsorption might similarly block or displace only a fraction of the exchangeable cations in montmorillonite. Francis (1973) reported that PVP adsorption by bentonites was largely irreversible in that 10 to 39 g of PVP/100 g of bentonite remained after multiple washes using a variety of solvents. Francis (1973) noted that nonionic polymer (*e.g.* PVP) adsorption is largely due to van der Waals forces.

Ricin is an ionic polymer and the proportion of negative and positive charge sites varies with solution pH. Many of the constituent amino-acid side-chains in ricin have alkyl or other neutral functional groups that might form van der Waals bonds with the siloxane surface. Hence, ricin adsorption to montmorillonite might involve a combination of van der Waal's and coulombic interactions.

Research by Norde (2003) differentiated the contributions of electrostatic and non-electrostatic bonding to protein adsorption to negatively charged surfaces. Norde (2003) showed that electrostatic forces dominated charged globular protein (lysozyme$^+$, α-lactalbumin$^-$) adsorption to polar, negatively charged silica surfaces with much greater lysozyme$^+$ adsorption. Yet, non-electrostatic forces dominated in adsorption to apolar, negatively charged polystyrene surfaces with greater α-lactalbumin$^-$ adsorption.

Dehydration of a clay/ricin complex might act to compress interlayer ricin molecules and bring more of the molecule into contact with the clay surface. Hence, it is likely that ricin could be more readily desorbed from hydrated clay/ricin complexes that have never been dried.

CONCLUSIONS

Ricin adsorption to two montmorillonites, a sepiolite, a palygorskite and a kaolinite yielded Langmuir-type isotherms. The monolayer ricin adsorption capacity of montmorillonite (444 g/kg) based on a Langmuir fit to the isotherm was many times greater than that for kaolinite (5.6 g/kg) at pH 7. At pH 5, the monolayer adsorption capacity of montmorillonite (694 g/kg) was ~1.5 times greater than at pH 7. These adsorption capacities were calculated using a ricin stock solution that also contained other proteins. Greater ricin adsorp-

https://doi.org/10.1346/CCMN.2005.0530306 Published online by Cambridge University Press

tion could be achieved using highly purified ricin. Ricin with an isoelectric point at pH 7.1 should be positively charged at pH 5 and negatively charged at pH 10. Ricin adsorption at pHs 4, 5 and 7 caused interlayer expansion of montmorillonite, but not at pH 10. Ricin adsorption paralleled both the CECs and surface areas of the clay mineral samples, but the pH effect suggests that cation exchange might drive adsorption. Through adsorption, clay minerals in soils and sediments might effectively mitigate the toxicity of dispersed ricin and smectites might be used directly for site cleanup.

ACKNOWLEDGMENTS

We thank the reviewers, Dr James Harsh and Dr Heather Dion, and Associate Editor Dr David Laird for comments and suggestions that greatly improved this manuscript. Access to Dr Necip Güven's X-ray diffractometer was greatly appreciated. College of Agricultural Sciences and Natural Resources Publication # T-4-553 funded by the Department of Defense under contract # DAAD-13-02-C0067.

REFERENCES

Boroda, E., Jaynes, W.F., Zartman, R.E., Green, C.J., San Francisco, M.J. and Zak, J.C. (2004) Enzyme-linked immunosorbent assay measurement of castor toxin in soils. *Communications in Soil Science and Plant Analysis*, **35**, 1185–1195.

Bouyoucos, G.J. (1962) Hydrometer method improved for making particle size analysis of soils. *Agronomy Journal*, **54**, 464–465.

Bradford, M.M. (1976) A refined and sensitive method for the quantitation of microgram quantities of protein utilizing the principle of protein-dye binding. *Analytical Biochemistry*, **72**, 248–254.

Brindley, G.W. (1980) Order-disorder in clay mineral structures. P.172 in: *Crystal Structures of Clay Minerals and their X-ray Identification* (G.W. Brindley and G. Brown editors). Monograph **5**, Mineralogical Society, London.

Carter, D.L., Mortland, M.M. and Kemper, W.D. (1986) Specific surface. Pp. 413–423 in: *Methods of Soil Analysis. Part I. Physical and Mineralogical Methods*, 2nd edition (A. Klute, editor). Soil Science Society of America, Madison, Wisconsin.

Ding, X. and Henrichs, S.M. (2002) Adsorption and desorption of proteins and polyamino acids by clay minerals and marine sediments. *Marine Chemistry*, **77**, 225–237.

Francis, C.W. (1973) Adsorption of polyvinylpyrrolidone on reference clay minerals. *Soil Science*, **115**, 40–54.

Franz, D.R. and Jaax, N.K. (1997) Ricin toxin. Chapter 32 in: *Medical Aspects of Chemical and Biological Warfare. Textbook of Military Medicine* (R. Zajtchuk, editor). Published by The Office of the Surgeon General, US Army, Falls Church, Virginia, USA.

Fu, L., Weckhuysen, B.M., Verberckmoes, A.A. and Schoonheydt, R.A. (1996) Clay intercalated Cu(II) amino acid complexes: synthesis, spectroscopy and catalysis. *Clays and Clay Minerals*, **31**, 491–500.

Fusi, P., Ristori, G.G., Calamai, L. and Stotzky, G. (1989) Adsorption and binding of protein on 'clean' (homoionic) and 'dirty' (coated with Fe oxyhydroxides) montmorillonite, illite and kaolinite. *Soil Biology and Biochemistry*, **21**, 911–920.

Garwood, G.A., Mortland, M.M. and Pinnavaia, T.J. (1983) Immobilization of glucose oxidase on montmorillonite clay: hydrophobic and ionic modes of binding. *Journal of Molecular Catalysis*, **22**, 153–163.

Goh, K.M. (1972) Amino acid levels as indicators of paleosols in New Zealand soil profiles. *Geoderma*, **7**, 33–47.

Hartley, M.R. and Lord, J.M. (1993) Structure, function and applications of ricin and related cytotoxic proteins. *Plant Biotechnology*, **3**, 210–239.

Hiemenz, P.C. (1986) *Principles of Colloid and Surface Chemistry.* Marcel Dekker, New York, pp. 398–407.

Jaynes, W.F. and Bigham, J.M. (1986) Multiple cation-exchange capacity measurements on standard clays using a commercial mechanical extractor. *Clays and Clay Minerals*, **34**, 93–98.

Jaynes, W.F. and Bigham, J.M. (1987) Charge reduction, octahedral charge, and lithium retention in heated, Li-saturated smectites. *Clays and Clay Minerals*, **35**, 440–448.

Jaynes, W.F. and Boyd, S.A. (1991) Clay mineral type and organic compound sorption by hexadecyltrimethylammonium-exchanged clays. *Soil Science Society of America Journal*, **55**, 43–48.

Katzin, B.J., Collins, E.J. and Robertus, J.D. (1991) The structure of ricin A chain at 2.5 Å. *Proteins: Structure, Function, and Genetics*, **10**, 251–259.

Liener, I.E. (1997) Plant lectins: properties, nutritional significance, and function. Pp. 31–43 in: *Antinutrients and Phytochemicals in Food* (F. Shahidi, editor). ACS Symposium Series **662**, American Chemical Society, Washington, D.C.

MacEwan, D.M.C. and Wilson, M.J. (1980) Interlayer and intercalation complexes of clay minerals. P. 203 in: *Crystal Structures of Clay Minerals and their X-ray Identification* (G.W. Brindley and G. Brown, editors). Monograph **5**, Mineralogical Society, London.

Merck (2001) *The Merck Index, An Encyclopedia of Chemicals, Drugs and Biologicals*. Merck Research Laboratories Division of Merck & Co., Inc. Whitehouse Station, New Jersey. p. 8290.

Montfort, W., Villafranca, J.E., Monzingo, A.F., Ernst, S.R., Katzin, B., Rutenber, E., Xuong, N., Hamlin, R. and Robertus, J.D. (1987) The three-dimensional structure of ricin at 2.8 Å. *Journal of Biological Chemistry*, **262**, 5398–5403.

Mortland, M.M. and Raman, K.V. (1968) Surface acidity of smectites in relation to hydration, exchangeable cation, and structure. *Clays and Clay Minerals*, **16**, 393–398.

Nicolson, G.L. and Blaustein, J. (1972) The interaction of Ricinus communis agglutinin with normal and tumor cell surfaces. *Biochimica Biophysics Acta*, **266**, 543–547.

Norde, W., editor (2003) Adsorption of (bio)polymers, with special emphasis on globular proteins. Pp. 285–311 in: *Colloids and Interfaces in Life Sciences*. Marcel Dekker, Inc., New York.

Olsnes, S. and Pihl, A. (1973) Different biological properties of the two constituent peptide chains of ricin, a toxic protein inhibiting protein synthesis. *Biochemistry*, **12**, 3121–3126.

Owens, D. (2000) *Hidden Evidence. Forty True Crimes and How Forensic Science Helped Solve Them*. Firefly Books, Inc., Buffalo, New York.

Perez-Castells, R., Alvarez, A., Gavilanes, J., Lizarbe, M.A., Martinez Del Pozo, A., Olmo, N. and Santaren, J. (1985) Adsorption of collagen by sepiolite. *Proceedings of the International Clay Conference, Denver, 1985*, pp. 359–362.

Rausell-Colom, J.A. and Fornes, V. (1974) Monodimensional fourier analysis of some vermiculite-l-ornithine^{+} complexes. *American Mineralogist*, **59**, 790–798.

Rausell-Colom, J.A. and Serratosa, J.M. (1987) Reactions of clays with organic substances. P. 392 in: *Chemistry of Clays and Clay Minerals* (A.C.D. Newman, editor). Monograph **6**, Mineralogical Society, London.

Rutenber, E., Katzin, B.J., Ernst, S., Collins, E.J., Mlsna, D., Ready, M.P. and Robertus, J.D. (1991) Crystallographic refinement of ricin to 2.5 Å. *Proteins: Structure, Function, and Genetics*, **10**, 240–250.

Sigma (2000) *Sigma 2000/2001 Catalog*. Sigma-Aldrich Company. P.O. Box 14508. St. Louis, Missouri 63178, USA, pp. 1477 and 2045.

Singer, A. (2002) Palygorskite and sepiolite. P. 563 in: *Soil Mineralogy with Environmental Applications* (J.B. Dixon and D.G. Schulze, editors). Published by the Soil Science Society of America, Madison, Wisconsin.

Stryer, L. (1975) Introduction to protein structure and function. Chapter 2 in: *Biochemistry*. W.H. Freeman & Company. San Francisco, CA.

Van Olphen, H. and Fripiat, J.J. (editors) (1979) *Data Handbook for Clay Materials and Other Non-metallic Minerals*. Pergamon Press, New York.

Villafranca, J.E. and Robertus, J.D. (1977) Crystallographic study of the anti-tumor protein ricin. *Journal of Molecular Biology*, **116**, 331–335.

Yu, C.H., Norman, M.A., Newton, S.Q., Miller, D.M., Teppen, B.J. and Schafer, L. (2000) Molecular dynamics simulations of the adsorption of proteins on clay mineral surfaces. *Journal of Molecular Structure*, **556**, 95–103.

(*Received 28 April 2004; revised 17 November 2004; Ms. 909; A.E. David A. Laird*)